Turkish Journal of Electrical Engineering and Computer Sciences

Volume 23 | Number 6 Article 12

1-1-2015

Fuzzy sliding mode control applied to a doubly fed induction generator for wind turbines

SID AHMED EL MEHDI ARDJOUN

Mohamed Abid

Turkish Journal of Electrical Engineering & Computer Sciences

http://journals.tubitak.gov.tr/elektrik/

Research Article

Turk J Elec Eng & Comp Sci
(2015) 23: 1673 – 1686

doi:10.3906/elk-1404-64

Fuzzy sliding mode control applied to a doubly fed induction generator for wind turbines

Sid Ahmed El Mehdi ARDJOUN*, Mohamed ABID
IRECOM Laboratory, Department of Electrical Engineering, Djillali Liabes University, Sidi Bel-Abbes, Algeria

Received: 04.04.2014 • **Accepted/Published Online:** 12.02.2015 • **Printed:** 30.11.2015

Abstract: In this paper an indirect vector control using fuzzy sliding mode control is proposed for a double-fed induction generator (DFIG), applied for a wind energy conversion system in variable speed. The objective is to independently control the active and reactive power generated by the DFIG, which is decoupled by the orientation of the flux. The sliding mode control finds its strongest justification for the problem concerning the use of a robust nonlinear control law for the model uncertainties. As far as the fuzzy mode control is concerned, it aims at reducing the chattering effect. The obtained results show the increasing interest of such control in this system

Key words: Doubly fed induction generator, fuzzy sliding mode control, indirect vector control, power control, variable speed

1. Introduction

In recent years, there has been an evolution of wind electrical energy production. This source of energy has developed importantly considering the diversity of the exploitable zones and the relatively beneficial cost [1].

Now most wind turbines are equipped with a double-fed induction generator (DFIG) due to noticeable advantages: the variable speed generation ($\pm 30\%$ around the synchronous speed), the decoupled control of active and reactive powers, the reduction of mechanical stresses and acoustic noise, the improvement of the power quality, and the low cost [2].

In the literature on DFIG control, different techniques have been used, among them indirect vector control with a PI controller. This technique offers some advantages: practical implementation, protection against the DFIG currents at high intensity, and operation of the DFIG as an active filter [3]. However, this technique of control loses its robustness and performance during the exposure of the DFIG to some constraints, such as the effects of parameter uncertainties (caused by heating, saturation, etc.) and the speed variation disturbance. In addition to these drawbacks, there is also the effect of coupling between the active and the reactive power [4].

To ensure the robustness and good performance of the indirect vector control using a PI controller, several approaches have been recently proposed. In [5], the authors proposed to optimize the gains of PI controllers by the genetic algorithm. In [6] and [7], the authors proposed an adaptive control with fuzzy and neuro-fuzzy logic to adjust the gains of PI controllers. Other approaches were adopted to change the PI controllers for other controllers, namely polynomial RST based on pole placement theory and linear quadratic Gaussian [4], sliding mode [8], second-order sliding mode [9], and fuzzy logic [10].

*Correspondence: elmehdi.ardjoun@univ-sba.dz

In this paper, fuzzy sliding mode control (FSMC) has been proposed. The use of the sliding mode control has proven to be very helpful. This is due to the simplicity of the implementation and the robustness against system uncertainties and external disturbances affecting the process [11]. The disadvantage of the sliding mode control is that the discontinuous control signal produces chattering. In order to reduce the chattering phenomenon, discontinuous control is substituted by fuzzy mode control.

This work is thus intended to design a control that could reject the disrupting effects of speed variation and the effects of parametric uncertainties, and that could eliminate the coupling effect.

The paper is organized as follows: first the wind energy conversion system is described. Second, the DFIG model and the indirect vector control strategy are studied. The FSMC of the DFIG is then developed and tested. Finally, some observations are given comparing the use of FSMC with the PI controller.

2. Description of a wind energy conversion system

The wind conversion system, which is shown in Figure 1, consists of a wind turbine, a gearbox, a DFIG, and converters.

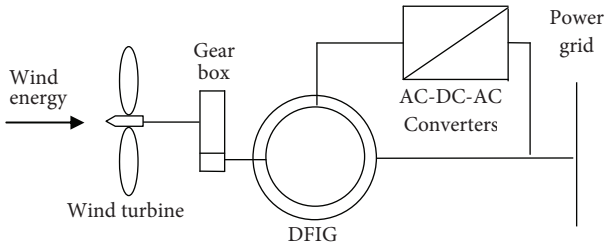

Figure 1. Scheme of energy transformation chain.

The wind is a result of pressure and temperature differences between several air areas unequally exposed to the sun. Its speed then depends on many meteorological phenomena and is consequently always fluctuating and not controllable [12].

The wind turbine converts the aerodynamic energy to mechanical energy. The total aerodynamic power available to the wind turbine is given by [13]:

$$P_{aer} = \frac{1}{2}\rho S\, v_w^3, \tag{1}$$

where ρ is air density (kg/m^3), S is turbine area (m^2), and v_w is wind speed (m/s).

However, only part of the supplied energy can be collected by the wind turbine [13]:

$$P_t = \frac{1}{2}\rho C_p S\, v_w^3, \tag{2}$$

where C_p is the power coefficient.

For the wind turbine, the power coefficient depends on the wind turbine's mechanical characteristics and is a function of the relative speed λ, which represents the ratio of the blade tip speed to the wind speed [13]:

$$\lambda = \frac{\omega_t\, R}{v_w}, \tag{3}$$

where ω_t is the angular frequency of the blades (rad/s) and $R$is the radius of the rotor blades (m).

For a given wind turbine and for a given wind speed, there is an optimum mechanical rotational speed that can produce a maximum mechanical power. To reach the latter we use the maximum power point tracking (MPPT) technique. In particular we employ the MPPT technique that is used in practice [14], known as power signal feedback. This method of adjustment uses the specifications of the wind turbine supplied by the manufacturer. These specifications are located in a table prerecorded in the control system, which provides for each rotation speed of the turbine a reference of maximum power production. This approach allows getting closer to the optimum using simple measures (without using a sensor for the wind speed). Such an approach also simplifies considerably the algorithm of the search for maximum power and uses the structures of more traditional and less expensive converters [15].

The gearbox enables us to increase the rotational speed of the generator and to reduce the torque [3].

The DFIG then converts this mechanical energy into electrical energy. If the losses are neglected, the total power delivered to the grid is the input mechanical power. This conversion is expressed by [1]:

$$P_t = (1+g)\,P_s, \tag{4}$$

where P_s is stator active power (W) and g is the DFIG slip.

The converters are used to transfer the maximum energy delivered by the wind turbine to the grid depending on the wind speed [3].

3. DFIG model and indirect vector control strategy

The modeling of the DFIG is described in the d-q Park reference frame. The following equation system describes the total generator model [3].

$$\begin{aligned} v_{ds} &= R_s i_{ds} + \tfrac{d\phi_{ds}}{dt} - \omega_s \phi_{qs} \\ v_{qs} &= R_s i_{qs} + \tfrac{d\phi_{qs}}{dt} + \omega_s \phi_{ds} \\ v_{dr} &= R_r i_{dr} + \tfrac{d\phi_{dr}}{dt} - \omega_r \phi_{qr} \\ v_{qr} &= R_r i_{qr} + \tfrac{d\phi_{qr}}{dt} + \omega_r \phi_{dr} \end{aligned} \tag{5}$$

$$\begin{aligned} \phi_{ds} &= L_s i_{ds} + M\, i_{dr} \\ \phi_{qs} &= L_s i_{qs} + M i_{qr} \\ \phi_{dr} &= L_r i_{dr} + M i_{ds} \\ \phi_{qr} &= L_r i_{qr} + M i_{qs} \end{aligned} \tag{6}$$

The mechanical equation is:

$$\Gamma_m = \Gamma_{em} + F\Omega + J\frac{d\Omega}{dt}. \tag{7}$$

The electromagnetic torque depends on d-q flux and the currents:

$$\Gamma_{em} = Np\frac{M}{L_s}\left(\phi_{qs} i_{dr} - \phi_{ds} i_{qr}\right), \tag{8}$$

where s,(r) are stator (rotor) subscripts, v,(i) are voltage (current), φ is flux linkage; R_r, (R_s) are rotor (stator) winding resistance per phase, L,(M) are self and mutual inductances for the equivalent stator and rotor

windings on the d- and q-axes, ω_r,(ω_s) are rotor (stator) electrical angular frequency, Γ_{em} is electromagnetic torque, Γ_m is mechanical torque, F is viscous torque coefficient, Ω is mechanical rotation in an angular frequency, J is global inertia, and N_p is number of pairs of poles.

To be able to easily control the production of electricity from the wind turbine, we will achieve independent control of active and reactive powers by establishing the equations that link the values of the rotor voltages, generated by a converter, to the stator active and reactive powers [3,4,14].

For obvious reasons of simplifications, the d-q reference frame related to the stator spinning field pattern and a stator flux aligned on the d-axis were adopted [9]. Consequently:

$$\phi_{ds} = \phi_s and \phi_{qs} = 0. \tag{9}$$

The electromagnetic torque of Eq. (8) becomes:

$$\Gamma_{em} = -Np\frac{M}{L_s}\phi_{ds} i_{qr}, \tag{10}$$

and the flux of Eq. (6) becomes:

$$\begin{array}{l} \phi_{ds} = L_s i_{ds} + M i_{dr} \\ 0 = L_s i_{qs} + M i_{qr} \end{array}. \tag{11}$$

Assuming that the grid is stable, this leads to a constant stator flux ϕ_s. In addition, the stator resistance can be neglected since it is a realistic assumption for generators used in the wind turbine. Based on these considerations, the following is obtained:

$$v_{ds} = 0, v_{qs} = v_s, and \phi_s = \frac{v_s}{\omega_s}. \tag{12}$$

Using Eq. (11), the link can be established between the stator and rotor currents:

$$\begin{array}{l} i_{ds} = -\frac{M}{L_s} i_{dr} + \frac{\phi_s}{L_s} \\ i_{qs} = -\frac{M}{L_s} i_{qr} \end{array}. \tag{13}$$

In the d-q reference frame, in an asynchronous generator stator, the active power P_s and reactive power Q_s delivered from the stator can be defined:

$$P_s = v_{ds} i_{ds} + v_{qs} i_{qs}, \tag{14}$$

$$Q_s = v_{qs} i_{ds} - v_{ds} i_{qs}. \tag{15}$$

The adaptation of these equations to the simplifying assumptions gives:

$$P_s = -v_s \frac{M}{L_s} i_{qr}, \tag{16}$$

$$Q_s = -v_s \frac{M}{L_s} i_{dr} + \frac{v_s^2}{L_s \omega_s}. \tag{17}$$

To be able to control the DFIG correctly, a relationship must be established between the rotor currents and the rotor voltages.

By substituting the stator currents of Eq. (13) in the equation of the flux (Eq. (6)), the following is obtained.

$$\begin{aligned}\phi_{dr} &= (L_r - \tfrac{M^2}{L_s})i_{dr} + \tfrac{MV_s}{L_s\omega_s} \\ \phi_{qr} &= (L_r - \tfrac{M^2}{L_s})i_{qr}\end{aligned} \tag{18}$$

By replacing the term of the rotor flux of the above equation (Eq. (18)) by their expressions in Eq. (5), the following is obtained.

$$v_{dr} = R_r i_{dr} + (L_r - \frac{M^2}{L_s})\frac{di_{dr}}{dt} - g(L_r - \frac{M^2}{L_s})\omega_s i_{qr} \tag{19}$$

$$v_{qr} = R_r i_{qr} + (L_r - \frac{M^2}{L_s})\frac{di_{qr}}{dt} + g(L_r - \frac{M^2}{L_s})\omega_s i_{dr} + g\frac{Mv_s}{L_s} \tag{20}$$

In a steady-state and from Eqs. (16), (17), (19), and (20), the following relationships can be established:

$$P_s = [v_{qr} - e_F - e_d]\left[\frac{1}{R_r + p\left(L_r - \frac{M^2}{L_s}\right)}\left(-\frac{M\,v_s}{L_s}\right)\right], \tag{21}$$

$$Q_s = [v_{dr} - e_q]\left[\frac{1}{R_r + p\left(L_r - \frac{M^2}{L_s}\right)}\left(-\frac{M\,v_s}{L_s}\right)\right], \tag{22}$$

where e_d and e_q are coupling terms between the d-q axis, and e_F represents the electromotive force dependent on the rotation speed. Thus, these terms are defined by:

$$e_d = g(L_r - \frac{M^2}{L_s})\omega_s i_{dr}, \quad e_q = g(L_r - \frac{M^2}{L_s})\omega_s i_{qr}, \quad e_F = g\frac{M}{L_s}\omega_s\phi_{sd}.$$

Eqs. (21) and (22) show the first-order transfer functions for both axes, linking the rotor voltages to the stator active and reactive power. They also show the influence of the coupling and the following error caused by the electromotive force.

To perform the power control of the DFIG, indirect vector control is applied. This control consists of reproducing in the reverse direction Eqs. (21) and (22) by imposing to the DFIG the rotor voltages to obtain the necessary powers.

However, the control has to take into account the influences of the coupling effect and the following error. This requires that each axis is controlled independently, each one with its own controllers (power controllers and rotor current controllers).

It should also be noted that the calculations of the controllers are based on assumed fixed parameters. However, in a real system, these parameters are subject to variations caused by different physical phenomena (inductors saturation, resistance heating, etc.). Identification of these parameters is also subject to inaccuracies due to the method and measuring devices.

To guarantee robustness and better performance of the indirect vector control, FSMC is proposed.

4. Sliding mode control

The basic idea of sliding mode control is first to draw the states of the system in an area properly selected, and then design a law command that will always keep the system in this region [16]. The sliding mode control goes through three stages, as follows.

4.1. Choice of switching surface

For a nonlinear system presented in the following form,

$$\dot{X} = h(X,t) + b(X,t)u(X,t), \tag{23}$$

or $X \in \Re^n$, $u \in \Re^m, h(X,t) \in \Re^n, b(X,t) \in \Re^{n\times m}_{,} h(X,t)$, $b(X,t)$ are two continuous and uncertain nonlinear functions, supposed to be limited.

The form of general equation given by Slotine and Li is taken to determine the sliding surface given by [17]:

$$S(X) = \left(\frac{d}{dt} + \delta\right)^{n-1} e, \tag{24}$$

where $e = X^d - X, X^d = \left[x^d, \dot{x}^d, x^d, ...\right]^T$, and e is the error on the signal to be adjusted, δ is a positive coefficient, n is the system order, X^d is the desired signal, and X is the state variable of the control signal.

4.2. Convergence condition

The convergence condition is defined by the Lyapunov equation [11]; it makes the area attractive and invariant.

$$S(X) \cdot \dot{S}(X) \leq 0 \tag{25}$$

4.3. Control calculation

The control algorithm is defined by the relation

$$u = u^{eq} + u^n, \tag{26}$$

where u is the control signal, u^{eq} is the equivalent control signal, u^n is the switching control term, and $sign(S(X))$ is a sign function.

$$u^n = u^{\max} sign(S(X)) \tag{27}$$

5. The sliding mode control application to the DFIG

This technique has been used to control the stator active power, the stator reactive power, and the rotor currents of a DFIG whose model is strongly coupled.

Commonly, in DFIG control using sliding mode theory, the surfaces are chosen according to the error between the reference input signal and the measured signals [16].

Considering that $e1, e2, e3$, and $e4$ are the errors of the active power, the reactive power, the quadrature rotor current, and the direct rotor current, respectively, we have the following.

$$\begin{bmatrix} e_1 \\ e_2 \\ e_3 \\ e_4 \end{bmatrix} = \begin{bmatrix} P_{sref} - P_s \\ Q_{sref} - Q_s \\ i_{qr}^{lim} - i_{qr} \\ i_{dr}^{lim} - i_{dr} \end{bmatrix} \tag{28}$$

If $n = 1$ is taken, the expression of the surfaces has the following form.

$$\begin{bmatrix} S(P) \\ S(Q) \\ S(i_{qr}) \\ S(i_{dr}) \end{bmatrix} = \begin{bmatrix} P_{sref} - P_s \\ Q_{sref} - Q_s \\ i_{qr}^{lim} - i_{qr} \\ i_{dr}^{lim} - i_{dr} \end{bmatrix} \tag{29}$$

By deriving the surfaces with the replacement of the term of the powers P_s and Q_s (Eqs. (16) and (17)), the following is obtained.

$$\begin{bmatrix} \dot{S}(P) \\ \dot{S}(Q) \\ \dot{S}(i_{qr}) \\ \dot{S}(i_{dr}) \end{bmatrix} = \begin{bmatrix} \dot{P}_{sref} + v_s \frac{M}{L_s} \dot{i}_{qr} \\ \dot{Q}_{sref} + v_s \frac{M}{L_s} \dot{i}_{dr} - \frac{v_s^2}{L_s \omega_s} \\ \dot{i}_{qr}^{lim} - \dot{i}_{qr} \\ \dot{i}_{dr}^{lim} - \dot{i}_{dr} \end{bmatrix} \tag{30}$$

The expressions of currents $\dot{i}_{qr}$ and $\dot{i}_{dr}$ are derived from the voltage equations v_{qr} and v_{dr} respectively (Eqs. (20) and (19)).

$$\begin{bmatrix} \dot{i}_{qr} \\ \dot{i}_{dr} \end{bmatrix} = \begin{bmatrix} -A\, i_{qr} - g\, \omega_s\, i_{dr} + \frac{1}{\sigma\, L_r}\, v_{qr} - \frac{M g\, v_s}{L_s\, L_r\, \sigma} \\ -\frac{1}{\sigma\, T_r}\, i_{dr} + g\, \omega_s\, i_{qr} + \frac{1}{\sigma\, L_r}\, v_{dr} \end{bmatrix} \tag{31}$$

Here, $A = \frac{1}{\sigma} \frac{1}{T_r}; T_r = \frac{L_r}{R_r}$; where σ is the leakage coefficient $[\sigma = 1 - M^2 / L_s L_r]$.

We replace the calculated $\dot{i}_{qr}$ and $\dot{i}_{dr}$ in Eq. (30).

$$\begin{bmatrix} \dot{S}(P) \\ \dot{S}(Q) \\ \dot{S}(i_{qr}) \\ \dot{S}(i_{dr}) \end{bmatrix} = \begin{bmatrix} \dot{P}_{sref} + v_s \frac{M}{L_s} (- A\, i_{qr} - g\, \omega_s\, i_{dr} + \frac{1}{\sigma\, L_r}\, v_{qr} - \frac{M g\, v_s}{L_s\, L_r\, \sigma}) \\ \dot{Q}_{sref} + v_s \frac{M}{L_s} (- \frac{1}{\sigma\, T_r}\, i_{dr} + g\, \omega_s\, i_{qr} + \frac{1}{\sigma\, L_r}\, v_{dr}) - \frac{v_s^2}{L_s \omega_s} \\ \dot{i}_{qr}^{lim} + A\, i_{qr} + g\, \omega_s\, i_{dr} - \frac{1}{\sigma\, L_r}\, v_{qr} + \frac{M g\, v_s}{L_s\, L_r\, \sigma} \\ \dot{i}_{dr}^{lim} + \frac{1}{\sigma\, T_r}\, i_{dr} - g\, \omega_s\, i_{qr} - \frac{1}{\sigma\, L_r}\, v_{dr} \end{bmatrix} \tag{32}$$

Here, i_{qr}, i_{dr}, v_{qr}, and v_{dr} are the control vectors, in order to force the path of the system to converge to the surfaces.

$$\begin{bmatrix} i_{qr} \\ i_{dr} \\ v_{qr} \\ v_{dr} \end{bmatrix} = \begin{bmatrix} i_{qr}^{eq} + i_{qr}^{n} \\ i_{dr}^{eq} + i_{dr}^{n} \\ v_{qr}^{eq} + v_{qr}^{n} \\ v_{dr}^{eq} + v_{dr}^{n} \end{bmatrix} \tag{33}$$

By replacing the expressions of the control vectors by their values in Eq. (32), the commands appear clearly in the following equation.

$$\begin{bmatrix} \dot{S}(P) \\ \dot{S}(Q) \\ \dot{S}(i_{qr}) \\ \dot{S}(i_{dr}) \end{bmatrix} = \begin{bmatrix} \dot{P}_{sref} + v_s \frac{M}{L_s}(- A(i_{qr}^{eq} + i_{qr}^{n}) - g\,\omega_s\, i_{dr} + \frac{1}{\sigma\, L_r}\, v_{qr} - \frac{Mg\, v_s}{L_s\, L_r\, \sigma}) \\ \dot{Q}_{sref} + v_s \frac{M}{L_s}(- \frac{1}{\sigma\, T_r}(i_{dr}^{eq} + i_{dr}^{n}) + g\,\omega_s\, i_{qr} + \frac{1}{\sigma\, L_r}\, v_{dr}\,) - \frac{v_s^2}{L_s \omega_s} \\ \dot{i}_{qr}^{lim} + A\, i_{qr} + g\,\omega_s\, i_{dr} - \frac{1}{\sigma\, L_r}(v_{qr}^{eq} + v_{qr}^{n}) + \frac{Mg\, v_s}{L_s\, L_r\, \sigma} \\ \dot{i}_{dr}^{lim} + \frac{1}{\sigma\, T_r}\, i_{dr} - g\,\omega_s\, i_{qr} - \frac{1}{\sigma\, L_r}(v_{dr}^{eq} + v_{dr}^{n}) \end{bmatrix} \tag{34}$$

During the sliding mode and in steady state, the values of the sliding surface, the derivative of the sliding surface, and the switching control are equal to zero.

The equivalent controls are found from Eq. (34) and written as follows.

$$\begin{bmatrix} i_{qr}^{eq} \\ i_{dr}^{eq} \\ v_{qr}^{eq} \\ v_{dr}^{eq} \end{bmatrix} = \begin{bmatrix} \frac{L_s}{A\, v_s\, M}\dot{P}_{sref} - \frac{g\,\omega_s}{A}\, i_{dr} + \frac{1}{A\sigma\, L_r}\, v_{qr} - \frac{Mg\, v_s}{R_r\, L_s} \\ \frac{\sigma\, T_r\, L_s}{v_s\, M}\dot{Q}_{sref} + g\,\omega_s\,\sigma\, T_r\, i_{qr} + \frac{T_r}{L_r}\, v_{dr} - \frac{\sigma\, T_r\, v_s}{M\omega_s} \\ \sigma\, L_r(\dot{i}_{qr}^{lim} + A\, i_{qr} + g\,\omega_s\, i_{dr}) + \frac{Mg\, v_s}{L_r} \\ \sigma\, L_r(\dot{i}_{dr}^{lim} + \frac{1}{\sigma\, T_r}\, i_{dr} - g\,\omega_s\, i_{qr}) \end{bmatrix} \tag{35}$$

During the convergence mode, so that the condition $S(X)\dot{S}(X) \leq 0$ is verified, the following is set.

$$\begin{bmatrix} \dot{S}(P) \\ \dot{S}(Q) \\ \dot{S}(i_{qr}) \\ \dot{S}(i_{dr}) \end{bmatrix} = \begin{bmatrix} -\frac{AMv_s}{L_s} i_{qr}^{n} \\ -\frac{Mv_s}{\sigma\, T_r\, L_s} i_{dr}^{n} \\ -\frac{1}{\sigma\, L_r} v_{qr}^{n} \\ -\frac{1}{\sigma\, L_r} v_{dr}^{n} \end{bmatrix} \tag{36}$$

Consequently, the switching terms are given by the following.

$$\begin{bmatrix} i_{qr}^{n} \\ i_{dr}^{n} \\ v_{qr}^{n} \\ v_{dr}^{n} \end{bmatrix} = \begin{bmatrix} Ki_{qr} sign(S(P)) \\ Ki_{dr} sign(S(Q)) \\ Kv_{qr} sign(S(i_{qr})) \\ Kv_{dr} sign(S(i_{dr})) \end{bmatrix} \tag{37}$$

To verify the system stability condition, parameters Ki_{qr}, Ki_{dr}, Kv_{qr}, and Kv_{dr} must be positive.

To reduce any possible overshoot of currents i_{qr} and i_{dr}, it is often useful to add current limiters.

$$\begin{bmatrix} i_{qr}^{lim} \\ i_{dr}^{lim} \end{bmatrix} = \begin{bmatrix} i_{qr}^{max} sat(i_{qr}) \\ i_{dr}^{max} sat(i_{dr}) \end{bmatrix} \tag{38}$$

6. Fuzzy sliding mode control

FSMC is a hybrid development of sliding mode control and fuzzy logic control, where the switching controller term, K sign($S(X)$), has been replaced by an inference fuzzy system [18].

$$u = u^{eq} + u^{fuzz} \tag{39}$$

For the input variables (sliding surface) and for the output variables (i_{qr}^{fuzz}, i_{dr}^{fuzz}, v_{qr}^{fuzz}, v_{dr}^{fuzz}), the fuzzy sets have been defined as follows: NB for negative big, NM for negative medium, EZ for zero, PM for positive medium, and PB for positive big.

Membership functions in triangular shape are shown in Figures 2 and 3. The rule base of the FSMC are shown in the Table.

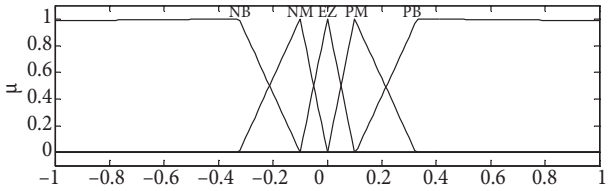

Figure 2. Membership functions for sliding surface.

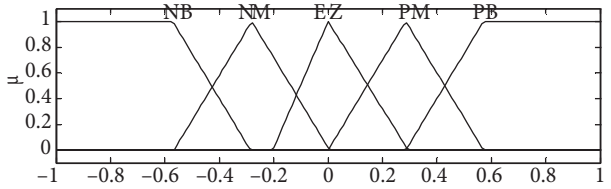

Figure 3. Membership functions for output variables.

Table. The rule base of the FSMC.

Fuzzy input	NB	NM	EZ	PM	PB
Fuzzy output	NB	NM	EZ	PM	PB

To reach the objective, a Mamdani-type fuzzy logic system is used, and the membership function of the resulting aggregation is established by maximum method. The defuzzification of the control output is achieved by adopting the centroid operator.

7. Obtained results

To demonstrate the performance and the robustness of the FSMC applied to a DFIG, we put it in the closest possible operating conditions to those of a wind system.

The active power is controlled to follow the reference power. The latter is adapted to the wind speed by the MPPT, whereas the reactive power control allows us to get a unitary power factor.

The parameters of the DFIG are as follows: $P_n = 20$ kW, $N_p = 2$, $R_s = 0.455\ \Omega$, $L_s = 0.07$ H, $R_r = 0.19\ \Omega$, $L_r = 0.0213$ H, $M = 0.034$ H, $F = 0.0024$ Nm/s, $J = 0.53$ kg m^2, and $R = 3.5$ m. In the case of parametric uncertainties, the resistance increases by 50% and the inductances decrease by 50%.

Figure 4 illustrates the proposed control system. The obtained results are shown in Figures 5–12.

The results clearly show the limits of the PI controller. Indeed, for this controller, the active power could not properly track its reference (following error), and the response of the reactive power is disrupted. We also notice that there is a random response of the DFIG rotational speed. All this is due to the speed variation and the coupling effect. With the parametric uncertainties, the following error and the reactive power disturbance increase, whereas with the FSMC, the active and the reactive powers follow their references perfectly. There is no coupling effect between the active power and reactive power, and thus no following error of the active power.

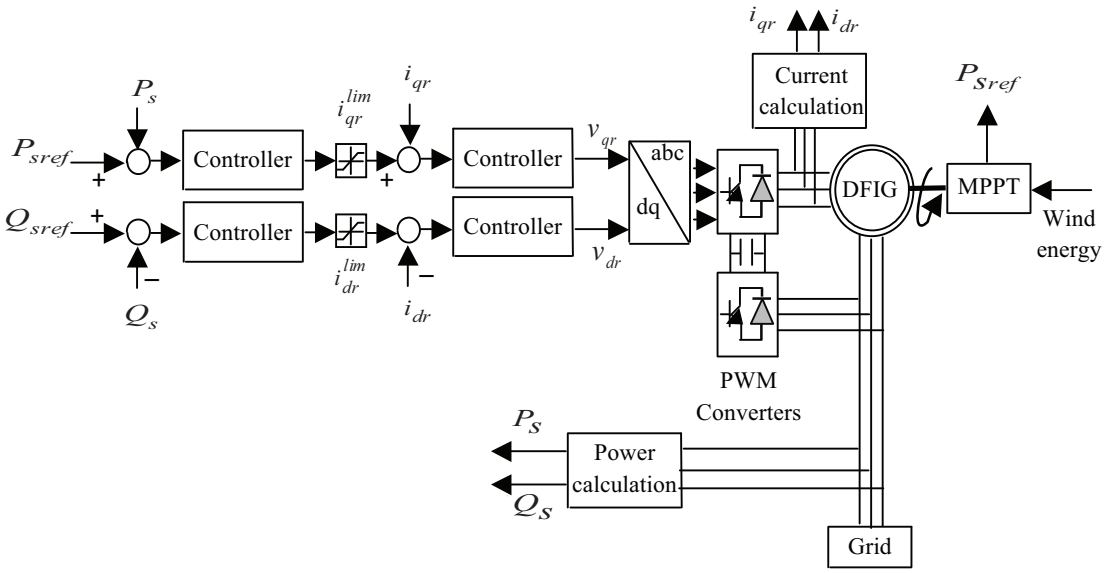

Figure 4. Block diagram of the proposed control system.

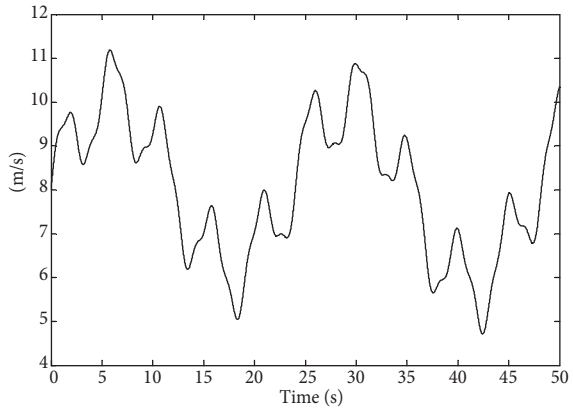

Figure 5. Wind speed evolution (m/s) versus time (s).

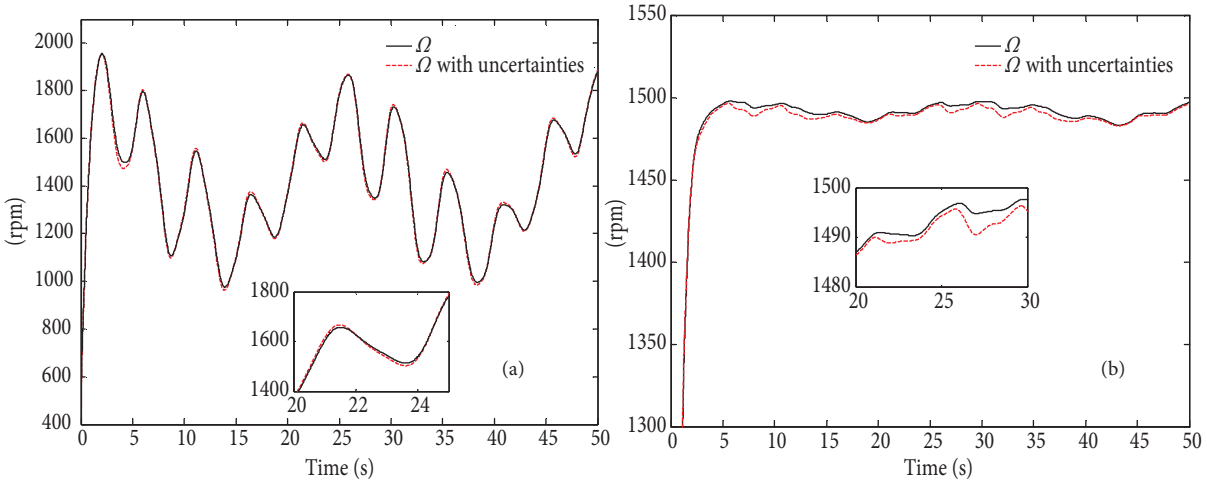

Figure 6. The responses of DFIG mechanical rotational speed: (a) with PI controller, (b) with FSMC.

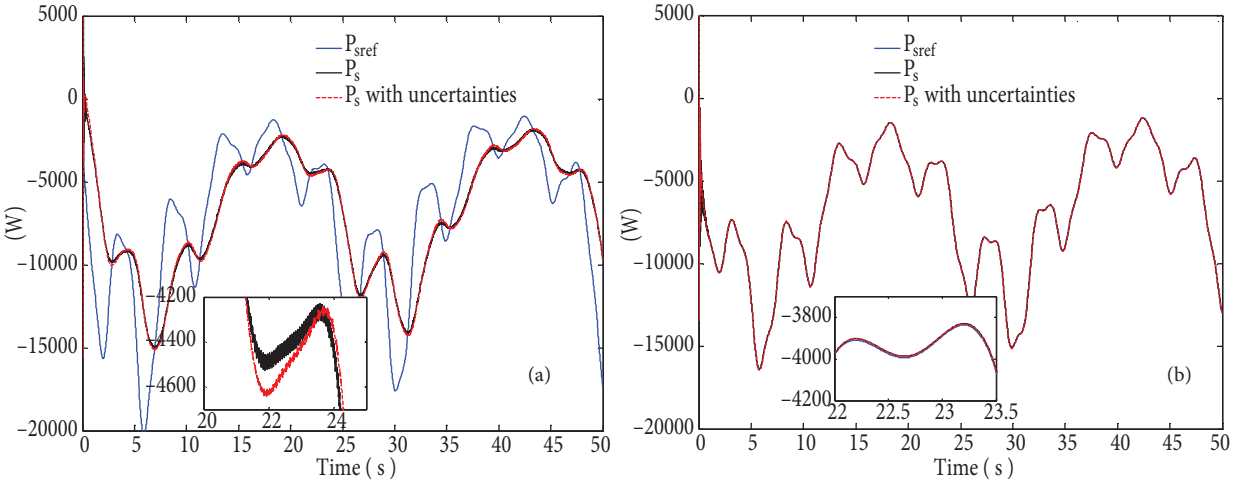

Figure 7. The responses of stator active power: (a) with PI controller, (b) with FSMC.

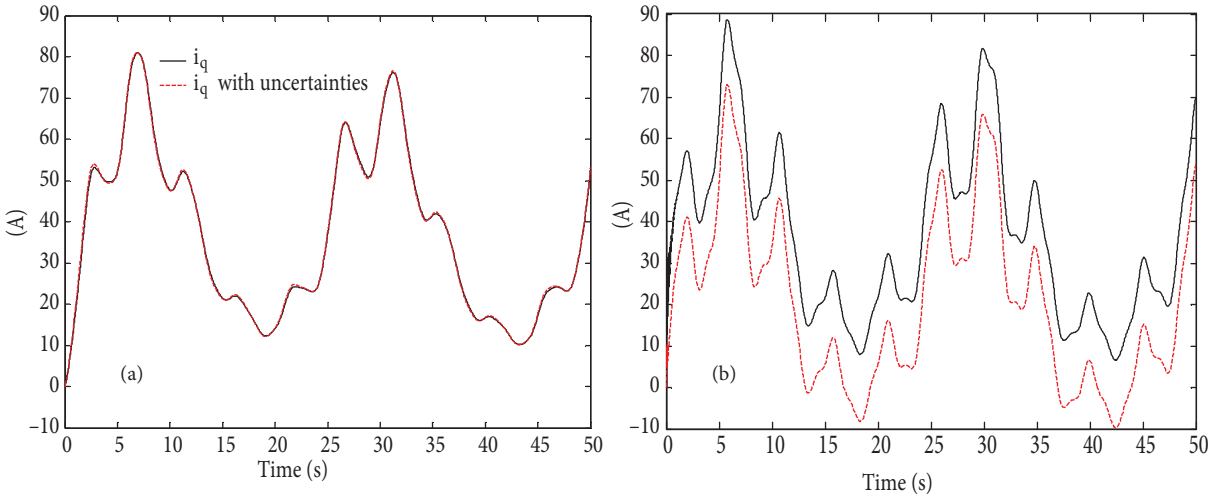

Figure 8. The responses of quadrature rotor current: (a) with PI controller, (b) with FSMC.

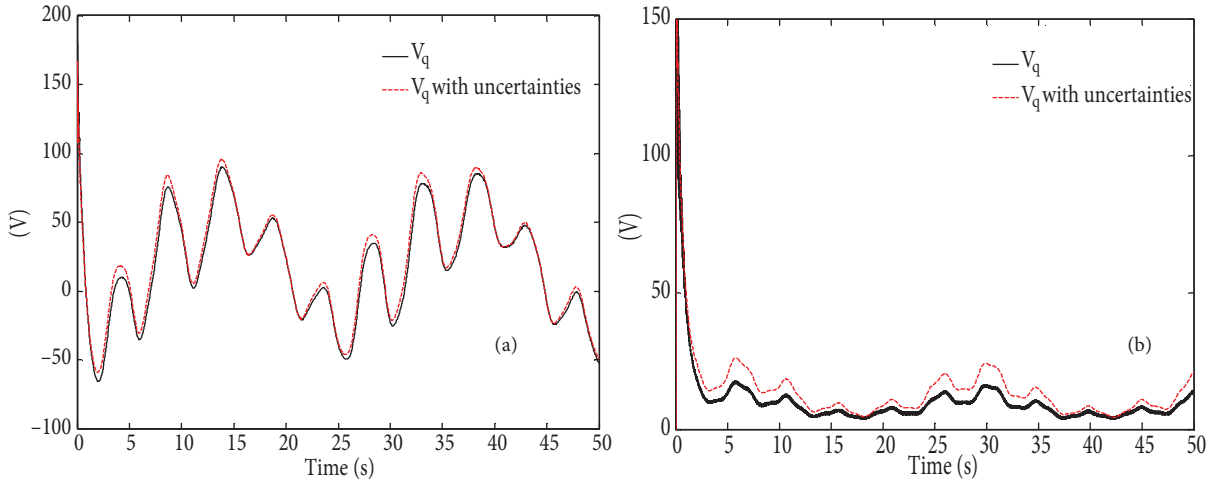

Figure 9. The responses of quadrature rotor voltage: (a) with PI controller, (b) with FSMC.

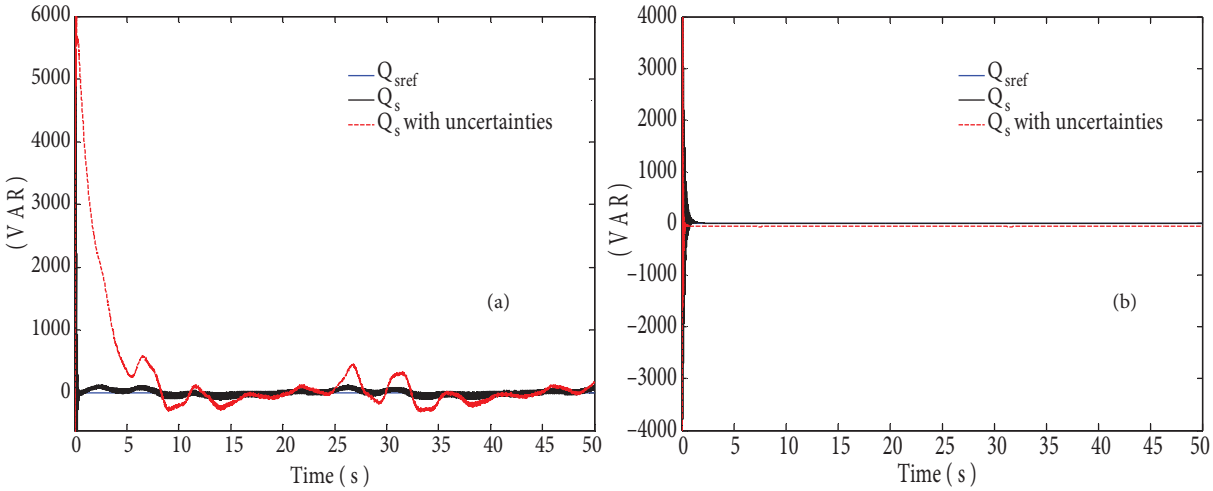

Figure 10. The responses of stator reactive power: (a) with PI controller, (b) with FSMC.

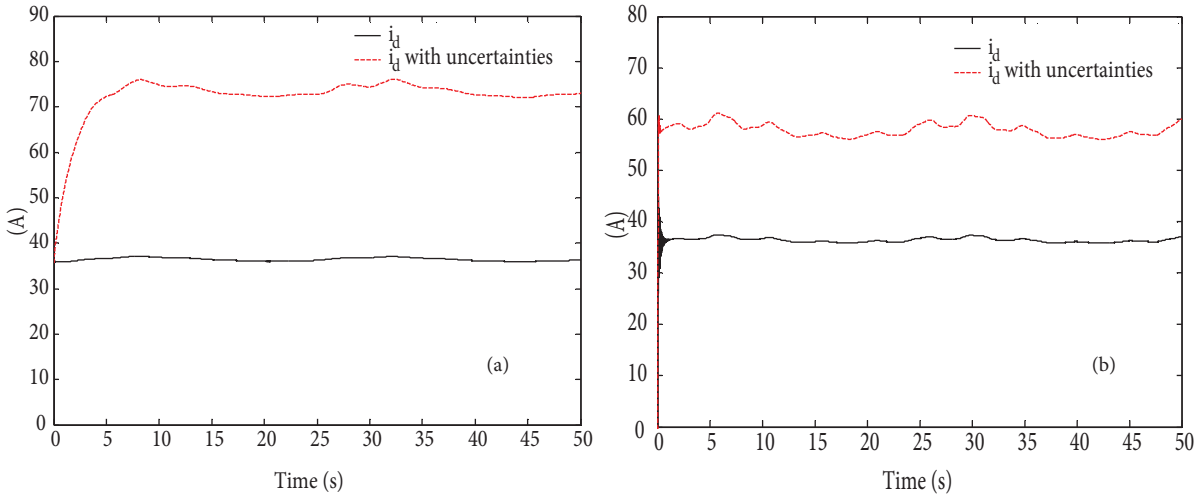

Figure 11. The responses of direct rotor current: (a) with PI controller, (b) with FSMC.

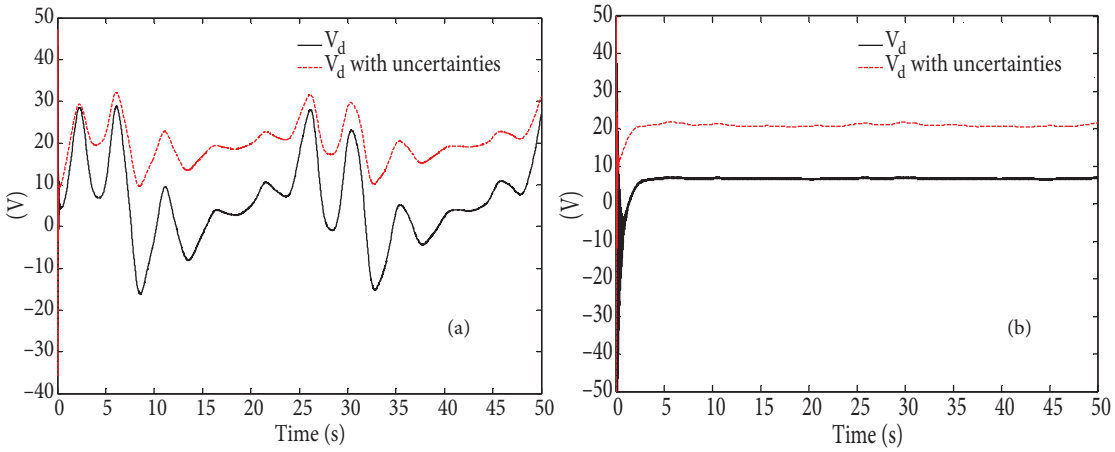

Figure 12. The responses of direct rotor voltage: (a) with PI controller, (b) with FSMC.

We can therefore say that the proposed controllers perfectly reject the disturbance of the speed variation (following error), the coupling effect, and the parametric uncertainties.

8. Conclusion

In the domain of wind energy conversion systems, the approach of adopting FSMC is of interest to improve the performance of the DFIG control.

The FSMC method is used for the active and reactive independent power control of a double-fed induction generator for variable-speed wind turbines using stator flux vector-oriented control.

After modeling the system, four controllers were developed using the fuzzy sliding mode (one for the active power, one for the reactive power, and two for the rotor currents).

With the appropriate choice of the parameter control, the obtained results are interesting for wind energy application to ensure robustness and better quality of the generated power when the speed is varying. Furthermore, this regulation presents a simple robust control algorithm that has the advantage of being easily implantable in calculators.

References

[1] Wu B, Lang Y, Zargari N, Kouro S. Power Conversion and Control of Wind Energy Systems. Hoboken, NJ, USA: John Wiley & Sons, 2011.

[2] Muller S, Deicke M, De Doncker RW. Doubly fed induction generator systems for wind turbines. IEEE Ind Appl Mag 2002; 8: 26–33.

[3] Boyette A. Contrôle-Commande d'une GADA avec Système de Stockage pour la Production Eolienne. PhD, Henry Poincaré University, Nancy, France, 2006 (in French).

[4] Poitiers F, Bouaouiche T, Machmoum M. Advanced control of a doubly-fed induction generator for wind energy conversion. Electr Pow Syst Res 2009; 79: 1085–1096.

[5] Nunes MVA, Vieira JPA, Bezerra UH. Designing optimal controllers for doubly fed induction generators using a genetic algorithm. IET Gener Transm Dis 2009; 3: 472–484.

[6] Hany MJ, Lakshmi VI, Chitradeep S, Narayan CK. Self-adjusting and fuzzy logic gain schedulers for vector control of wind driven doubly-fed induction generator. Int J Environ Stud 2012; 69: 299–313.

[7] Hany MJ, Dongyun L, Narayan CK. Design and implementation of neuro-fuzzy vector control for wind-driven doubly-fed induction generator. IEEE T Sustain Energ 2011; 2: 404–413.

[8] Ahmed MK, Khaled MH, Ali MY. Dynamic modeling and robust power control of DFIG driven by wind turbine at infinite grid. Electr Pow Energ Syst 2013; 44: 375–382.

[9] Abdeddaim S, Betka A. Optimal tracking and robust power control of the DFIG wind turbine. Electr Pow Energ Syst 2013; 49: 234–242.

[10] Fu HL, Thien HT. Modeling a wind turbine system using DFIG and realization of current control on the model with fuzzy logic controller. In: Zelinka I, Duy VH, Cha J, editors. Recent Advances in Electrical Engineering and Related Sciences. Berlin, Germany: Springer, 2014. pp. 85–92.

[11] Lopez P, Nouri AS. Théorie Elémentaire Et Pratique De La Commande Par Les Régimes Glissants. Berlin, Germany: Springer, 2006 (in French).

[12] Machmoum M, Poitiers F, Darengosse C, Queric A. Dynamic performances of a doubly-fed induction machine for a variable-speed wind energy generation. In: IEEE 2002 International Conference on Power System Technology, December 2002. New York, NY, USA: IEEE. pp. 2431–2436.

[13] Multon B, Roboam X, Dakyo B, Nichita C, Gergaud O, Ben Ahmed H. Aérogénérateurs électriques. Paris, France: Technique de l'Ingénieur, 2008 (in French).

[14] Aguglia D. Conception Globale des Générateurs Asynchrones à Double Alimentation pour Éoliennes. PhD, Laval University, Quebec, Canada, 2010 (in French).

[15] Koutroulis E, Kalaitzakis K. Design of a maximum power tracking system for wind-energy-conversion applications. IEEE T Ind Electron 2006; 53: 486–494.

[16] Utkin VI. Sliding mode control design principles and applications to electric drives. IEEE T Ind Electron 1993; 40: 23–36.

[17] Slotine JJE, Li W. Applied Nonlinear Control. Englewood Cliffs, NJ, USA: Prentice Hall, 1998.

[18] Wong LK, Leung FHF, Tam PKS. A fuzzy sliding controller for nonlinear systems. IEEE T Ind Electron 2001; 48: 32–37.